Journal of Research and Applications in Mechanical Engineering
ISSN: 2229-2152 (Print); 2697-424x (Online)
(2025) Vol. 13, No. 1, Paper No. JRAME-25-13-003
[DOI: 10.14456/jrame.2025.3]

Research Article

Design Procedure of an Axial Flow Irrigation Pump

K. Wasinarom[1]
J. Charoensuk[2]
W. Sanghirun[3]
S. Kaewnai[4]
M. Jaikuson[2,*]
[1] *School of International and Interdisciplinary Engineering Programs, School of Engineering, King Mongkut's Institute of Technology Ladkrabang, Bangkok 10520, Thailand*
[2] *Department of Mechanical Engineering, School of Engineering, King Mongkut's Institute of Technology Ladkrabang, Bangkok 10520, Thailand*
[3] *The Joint Graduate School of Energy and Environment, King Mongkut's University of Technology Thonburi, Bangkok 10140, Thailand*
[4] *Department of Mechanical Engineering, Faculty of Engineering, King Mongkut's University of Technology Thonburi, Bangkok 10140, Thailand*

Received 8 November 2023
Revised 21 March 2024
Accepted 4 April 2024

Abstract:
The paper presents the design procedure of an axial flow irrigation pump. It was designed to deliver a flow rate of 9,000 L/min with a head of 4 m at the Best Efficiency Performance point (BEP). The target hydraulic efficiency was 75%. It started with the preliminary design which predefined the inlet and outlet blade angle of the impeller and the stator vane using a triangular velocity diagram. After that, the other components in the pump system which are the inlet bell, duct, and trailing cone were constructed in the Computer Aided-Design (CAD) software. Then, the flow structure of the pump system was obtained using Computational Fluid Dynamics (CFD). The impeller blade channel, guide vane profile, and the flow channel throughout the pump system were improved to attain target efficiency. This was done by awareness of the development of high velocity (jet flow) and low velocity wake (wake flow) along the entire flow channel. The blade profile was adjusted to minimize wake region while the high jet velocity was reduced. By continuously improving the blade profile, the final version's hydraulic efficiency was 75.27%. The head was 5.68 m with the flow rate of 11,676 L/min.

Keywords: *Thai irrigation pump, Pump design, Pump preliminary design, Pump efficiency, Pump performance*

1. Introduction

Irrigation pump has been widely used in Thailand in agricultural activities for more than 60 years. The irrigation pump is designed for ease of manufacturing. The selling price is low. It is user-friendly and has minimal maintenance costs. However, Thai irrigation pump manufacturers had been facing many technical difficulties in pump design which resulted in low operational efficiency. The best efficiency performance (BEP) from the standard test rig for the sample pumps from many sellers in the Thai market is only in the range of 40 % to 50% [1, 2], in contrast with the industrial pumps which operate at around 80% efficiency at BEP. According to [3], Thai irrigation pump developer is interested in cooperation in the development of 10-inch diameter irrigation pump with the minimum BEP of 75%, operating at the flow rate of 9,000 L/min and at the delivered head of 4 m. The designed speed was specified at 1,450 revolutions per minute. The project included an improvement work of the test rig from the previous project according to the new project commitment, which was intended for performance testing service to support pump manufacturers in Thailand.

* Corresponding author: M. Jaikuson
E-mail address: monthon.ja@kmitl.ac.th

The works concerning impeller development in an international arena were found to date back to the 60's. For instance, Ikui [4] designed the axial flow pump with the 320 mm impeller. Several parameters that affected efficiency were investigated. His final design provided 70% efficiency at BEP. The performance curve for all operation ranges was presented in the dimensionless variables. Since early 2000, Computational Fluid Dynamics (CFD) has had a significant role in the impeller development process. Geerts [5] studied the design of an axial flow impeller. He tested the impeller performance and performed the CFD simulation at the impeller speed of 755 RPM, a flow rate of 302 liter/min, and the delivered head of 1.24 m. The developed test rig complied with ISO 3555. The BEP was at 75%. He used the CFD result to guide the detailed design process to maximize efficiency. Onitsuka et al. [6] studied the impeller and the stator vane design of the axial flow machine. He examined three different configurations of stator vanes. The maximum BEP was 78% for the "Arc stator" type. This was because of the less shear flow compared with the other two stator vanes. Singh and Nestmann [7] stated the importance of velocity triangles analysis during the very first phase of the pump design process. With this analysis, the inlet and the outlet blade angle could be obtained with the appropriate incidence angle for building up the delivered head. After that, CFD simulation could be employed to optimize the profile shape between the inlet and outlet of the blade to maximize the efficiency. Wang et al. [8] investigated the effect of the gap in an axial flow machine between the impeller and the stator vane. The impeller diameter was 300 mm. Pump operated at the impeller speed of 1,000 RPM, the water flow rate of 350 LPM, and the delivered head of 4.6 m. They found that the maximum efficiency was 85% with a gap of 10 mm. Qian et al. [9] studied the effect of stator vanes angle. The pump had a 300 mm impeller diameter with 3 blades operating with a 5-blade stator vane. The designed speed was 1450 RPM. The obtained flow rate was 0.33 m^3/s. From the investigation, the maximum efficiency was 80% at BEP. The CFD was used as a tool in the design process.

According to the given literature, there have been several attempts to improve the pump performance. However, this paper focuses on the target flow and head with a given driving speed. It started with the preliminary design process and employment of the former available tested data with similarity laws. Firstly, the designer selected a pump type that suits the required head and flow rate using the specific speed determined by the targeted operating condition (Impeller speed is usually defined by a specified prime mover such as the motor or engine). The impeller diameter was then obtained by dimensional analysis. For the detailed design of the impeller, with the predefined speed and diameter, the blade inlet and outlet velocity triangles could be obtained at various specific radii of the impeller blade from hub to tip with the assumption of uniform flow. The blade shape, the inlet, and the outlet angles were then constructed in Computer Aided-Design (CAD) software. CFD was employed at this stage to verify the pump performance which may involve iteration to achieve the targeted design values.

This paper focuses on the design process of a 10-inch irrigation pump to meet the targeted efficiency while maintaining the simplicity of the flow channel for the benefit of minimum manufacturing cost. Given the targeted delivered head and flow at 4 m and 9000 m^3/s respectively with an energy efficiency not less than 75%, the design flow chart and simulation result, especially the velocity contour that were found related to hydraulic efficiency, will be discussed below.

2. Design Procedure

The design process was divided into preliminary design and blade profile design as shown in Fig. 1. All parameters except the blade profile were obtained in the preliminary design. The expected hydraulic efficiency was assumed during the preliminary design. The hydraulic efficiency was then obtained in detailed flow field simulation (CFD) which was carried out in blade profile design process. CFD was employed to optimize the blade profile until the expected efficiency was achieved. This involved an iterative method until the hydraulic efficiency of the final design of the impeller met the design objective.

The preliminary design process was carried out according to the given operating condition in Table 1. The general parameters of the pump were identified. The hub diameter and the operation speed were given according to the available prime mover and available gear set, and the strength of the structure of the system. The design process was focused on the operation at the BEP. Then, the dimensionless specific speed was calculated. The calculated specific speed suggested the appropriate pump type which in this case, was the axial flow machine.

After that, the triangular velocity of the impeller blade was constructed (Fig. 2). The triangular velocity at the leading edge can be defined by vector $\mathbf{U_1}$ and vector $\mathbf{C_{x1}}$. The magnitude of a vector $\mathbf{C_{x1}}$ can be calculated by the designed flow rate (Q) and the annulus flow cross-sectional area (Eq.(1)). The magnitude of vector $\mathbf{U_1}$ can be defined by the angular velocity of the impeller and the span-wise radius from the shaft (Eq.(2)). All the information needed can be obtained in the predefined parameter in Table 1. To analyze the triangular velocity at the trailing edge, vector $\mathbf{U_2}$ was defined by the same method as vector $\mathbf{U_1}$. Since the blade velocity varied from the impeller root to the tip (outside diameter). The velocity triangle analysis was varied for four different radii from the hub radius to the outside diameter of the impeller blade which was the hub radius (blade root), average radius, mean radius, and outer radius as shown in Fig. 3. The equation used to calculate average radius and mean radius are Eq.(6) and Eq.(7). The incident angle at the leading edge was predefined by the designer and will be fine-tuned in CFD. The small incident angles helped build up the delivered head while maintaining the low shear flow structure along the impeller channel. Excessive incident angle design resulted in flow separation which was the main source of energy dissipation. To calculate the trailing edge beta angle (β2) along four different radii, the process began with torque prediction from Eq.(3). The theoretical head (H), predefined shaft speed, and the assumed hydraulic efficiency were available in Table 1. Then, the distribution of the swirling velocity component at the trailing edge was assigned to achieve the free vortex flow structure at the trailing edge as they must have a linear relation with radii from the shaft center. The C_{u2} profile could be obtained by Eq.(4) and Eq.(5). The obtained beta angles at the trailing edge were listed in Table 2. The free vortex swirling pattern at the impeller trailing edge along the impeller radius was designed to exhibit irrotational swirling flow behind the impeller. This was done to minimize dissipation since there was a gap between the trailing edge of the impeller and the stator vane where swirling kinetic energy could be recovered. For the stator vane, the triangular velocity diagram was applied at the vane inlet. The inlet angle of the vane was designed to coincide with the incoming swirling flow from the impeller. The vane exit blade angle would be 90 degrees implying that the exit flow was in the axial direction. Finally, the beta angle of each radius at the leading edge, the trailing edge of the impeller, and the inlet angle of the stator vane were obtained (Table 2).

In a preliminary analysis, all operation parameters can be estimated except the blade profile and the hydraulic efficiency. The blade profile is usually optimized by Computational Fluid Dynamics (CFD). The CFD allows designers to explore detailed flow fields inside the pump where the amount of viscous dissipation (entropy generation) can be quantified at the specific area. Then, the blade profile optimization is carried out repeatedly to reduce the overall rotational flow in the pump. The final version pump system is shown in Fig. 4. (In reality, there is around 20% of viscous dissipation taking place in the pump operating at BEP if the blade profile is optimized to minimize the rotational flow inside the pump.)

Table 1: Predefined parameters at BEP

Speed	1,450 RPM
Impeller diameter	10 inch
Deliver head	4 m
Flow rate	9,000 L/min
Hub diameter	102 mm
Estimate hydraulic efficiency	75%
Number of blades	4
Calculated specific speed (SI units)	1,588.39

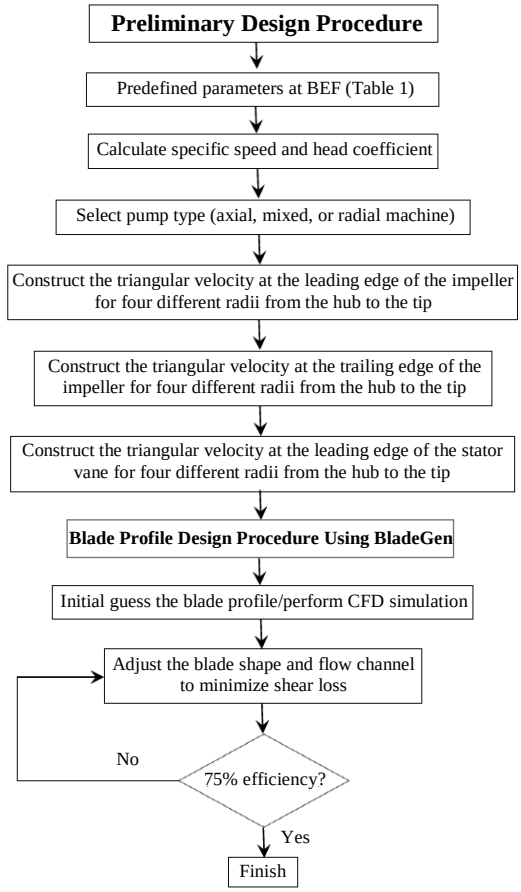

Fig. 1. Design procedure of irrigation pump system

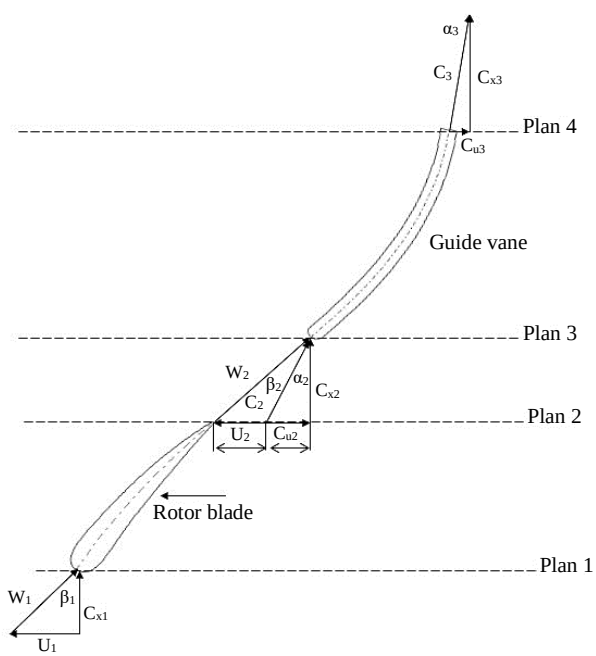

Fig. 2. Triangular velocity diagrams at the impeller and guide vane's inlets and outlets

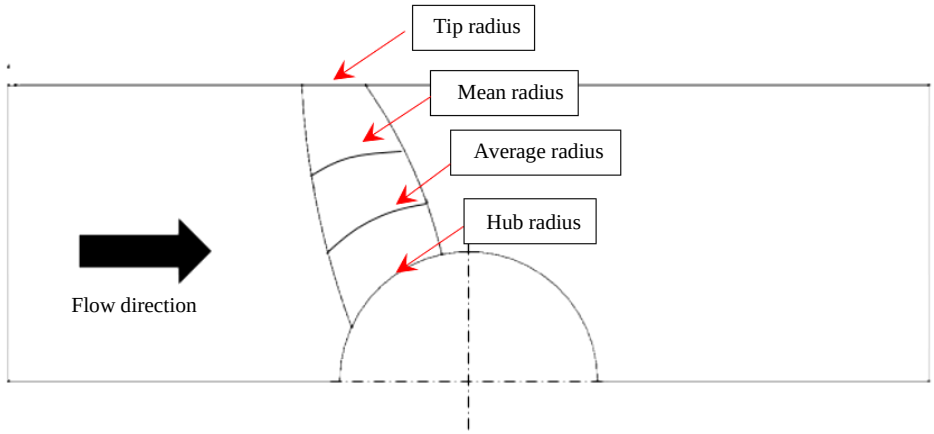

Fig. 3. Four different locations on the impeller blade

Table 2: Preliminary design result of impeller blade

Incident angle design	2	degree
LE Impeller angle at hub radius	40	degree
LE Impeller angle at average radius	17.50	degree
LE Impeller angle at mean radius	15	degree
LE Impeller angle at tip radius	11	degree
TE Impeller angle at hub radius	58.96	degree
TE Impeller angle at average radius	18.48	degree
TE Impeller angle at mean radius	16.32	degree
TE Impeller angle at tip radius	11.47	degree
LE Stator vane angle at hub radius	38	degree
LE Stator vane angle at average radius	42.30	degree
LE Stator vane angle at mean radius	53	degree
LE Stator vane angle at tip radius	62.20	Degree

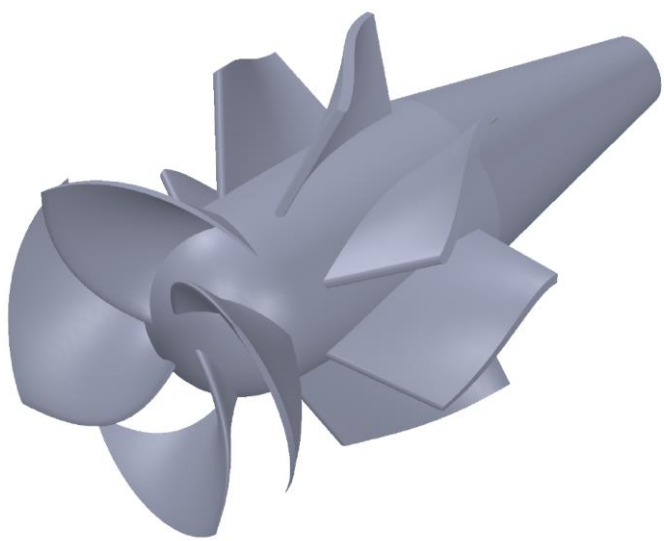

Fig. 4. Final version pump system

3. Calculation Parameters

From Fig.1, the magnitude of a vector C_{x1} from can be calculated by the designed flow rate (Q) and the annulus flow cross-sectional area as written below.

$$C_{x1} = \frac{4Q}{\pi(d_i^2 - d_h^2)} \tag{1}$$

The magnitude of vector U_1 can be calculated by the equation below.

$$U_1 = \omega R \tag{2}$$

The hydraulic efficiency can be determined by the increasing in flow power between inlet and the outlet divided by input shaft power which can be expressed as

$$\eta = \frac{P_{output}}{P_{input}} = \frac{\rho g Q H}{2\pi n T} \tag{3}$$

Torque can be calculated from summation of the angular momentum change of swirling component at each radius location from hub to tip which can be written as

$$T = \rho \sum_{hub}^{tip} (Q_R C_{u2} R) \tag{4}$$

To obtain free vortex swirling flow structure behind the impeller, C_{u2} can be written as

$$C_{u2} R = Const \tag{5}$$

The mean diameter along the axial location of the blade can be calculated by

$$d_m = \sqrt{\frac{d_i^2 + d_a^2}{2}} \tag{6}$$

The average diameter along the axial location of the pump can be calculated by

$$d_{av} = \frac{d_i + d_a}{2} \tag{7}$$

4. CFD Modeling

The impeller and stator blade geometry were built using BladeGen software. The preliminary design parameters were employed in the initial version. The additional inlet bell with the inlet guide vane before the impeller and the trailing cone behind the stator vane were built in the model (Fig. 5). The complete geometry model of the pump system is imported to ANSYS R1 software where the CFD simulation will be performed. The tetrahedral mesh with the inflation layer was used in this simulation (Fig. 6). The mass flow rate was set as the inlet boundary condition. The static pressure of 0 Pascal (gauge pressure) was set as the outlet boundary condition. The Reynolds Averaged Navier-Stokes equations (RANS) with the k-ω SST turbulence closure were modeled in this work. The iterative SIMPLE algorithm was employed to solve the pressure and velocity field. The normalized residual was set at 10^{-4} for the convergent criteria. The k-ω SST turbulent model was selected because it has superior accuracy of hydrodynamics force prediction compared to the conventional standard k-ε turbulent model. The maximum Y+ values were less than 40 for all simulation cases. This indicated that the first control volume was located on the log layer of the boundary. The excessive Y+ value will reduce the accuracy of the separation flow location which is the key parameter of hydrodynamics force prediction. The model information was shown in Fig. 5. The model validation had been made

with the experimental result from the project standard test rig [3]. The validation using the same turbulent model with this work with the same order of Y+ value. The predicted and experimental results showed the average efficiency discrepancy of 5% for the entire operation range.

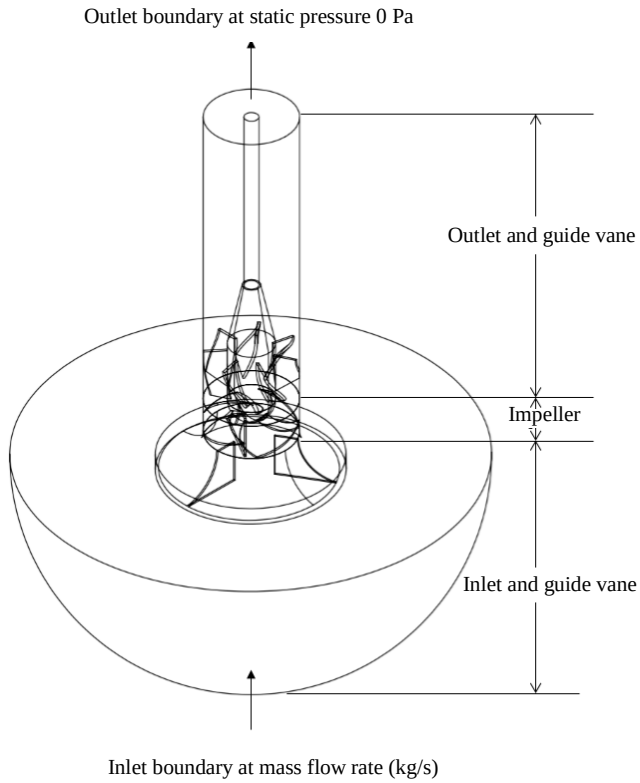

Fig. 5. Computational domain and boundary condition

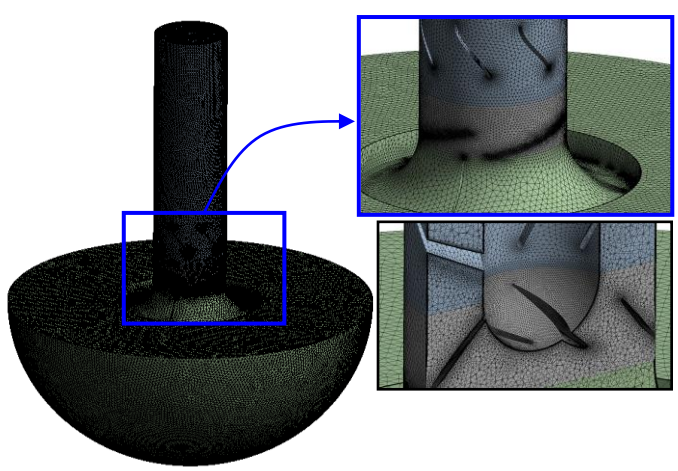

Fig. 6. Mesh and the inflation layer

5. Final Version CFD Performance

In a preliminary analysis, all operation parameters could be defined except the blade profile and the hydraulic efficiency which was later obtained in the blade profile design process. In the blade profile design procedure, CFD simulation was used as a tool to obtain detailed flow structure in the pump. The blade profile was optimized approaching the ideal uniform flow structure within the impeller and the stator vane channels. The high-velocity gradient flow structures (jet-wake, recirculation, secondary flow, separation flow) were pointed out and eliminated by adjusting the channel profile since it was the major source of energy dissipation (Internal Irreversibility). The impeller blade profile was also designed to obtain a free vortex flow structure behind the impeller because it was the ideally-zero dissipation swirling flow structure. The design process of the blade profile was carried out by iterative method as shown in Fig. 2. From the simulation result, the designer had paid attention to the slowing (wake) flow and the high-speed (jet) region along the entire flow channel. The development of the wake region usually ends up with a high dissipation separation flow. The wake region was alleviated by adjusting the blade profile to reduce the flow area to promote the stream tube pattern. On the other hand, the jet region was reduced by expanding the flow cross-section area. The improvement was repeated until the model reached the target efficiency (75%).

Even though, the design procedure was made at the BEP. All operation head and performance were simulated to construct the performance curve as shown in Fig. 7(a) and Fig. 7(b). This was done by varying the flow rate at the inlet boundary condition. From the converged CFD solution, the shaft torque can be obtained by summation of the pressure acting on the impeller blades. Then, the efficiency was calculated by Eq.(3). The delivery head can be calculated by the averaged total pressure difference between the inlet and the outlet boundary condition area (Fig. 5). The BEP point occurred at the flow rate of 11,676 L/min with a hydraulic efficiency of 75.27%. The delivered head was 5.68 m. The CFD result showed that the designed pump was able to achieve an efficiency of over 70% for the flow rate range of 0.17 to 0.21 m^3/s with the delivery head range from 4 to 7 m.

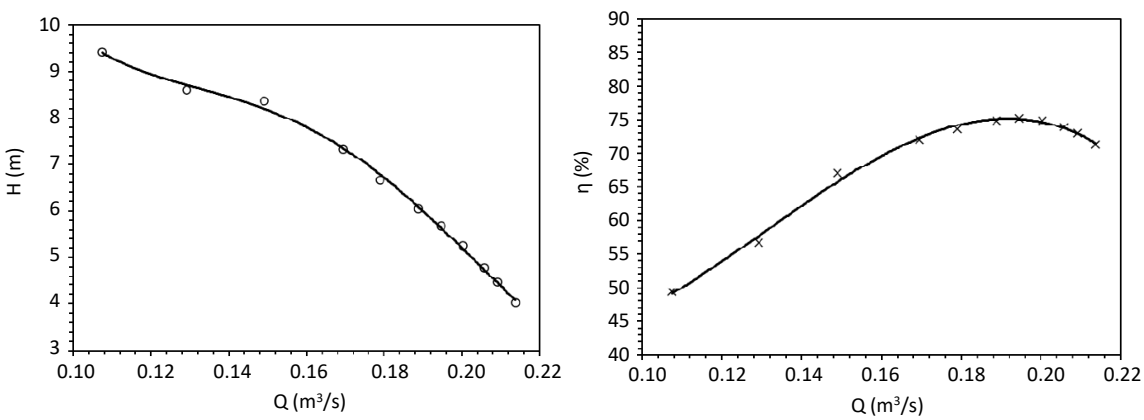

(a) H-Q curve (b) Efficiency-Q curve

Fig. 7. Head and efficiency curve

The efficiency of the pump depended on the flow field along the pump system. There had been many improvement focus on improving the flow field inside the pump [10, 11]. Entropy was the thermodynamics property that indicated amount of energy dissipation in the flow channel. There were a lot of researchers who improved energy performance of the pump based on the entropy generation distribution analysis along all pump components [12]. This paper focused on the flow structure obtained from CFD along the entire pump components starting from the inlet bell, impeller, stator vane, and the trailing cone. The analysis was addressed only on the final pump version obtained from the design process and operating at BEP. Fig. 8(a) shows the velocity magnitude along the pump system. The flow velocity gradually increased in the inlet bell as the flow cross area was reduced. The uniform flow structure was observed at the impeller inflow region. This confirmed that the impeller had received good quality flow. The flow velocity was abruptly changed in the impeller because of the swirling flow components created with the moving referenced frame (MRF) at the rotating impeller. High velocity was observed at a gap between the impeller and the stator vane as the high swirling flow components were induced by the rotating impeller. The swirling flow components had decreased

after the stator vane as the low velocity was observed. This indicated that the swirling kinetic energy was recovered in the stator vane. The swirling kinetic energy was converted to static pressure in the stator vane. A mild shear layer was observed at the trailing cone of the pump as shown in Fig. 8(b). This was because the simplified trailing cone profile as a straight cone rather than the optimized curve in the industrial pump. This simplification would result in little efficiency being incurred. However, this traded off with the lower manufacturing cost which kept the selling price reasonable for Thai irrigation pump market. Fig. 9(a) illustrated the minor jet-wake flow structure in the impeller channel. The area around the impeller tip had higher velocity than the region around the impeller hub. This was due to the higher induced swirling motion from the impeller tip speed compared with the lower blade speed around the hub region. Fig. 9(b) showed that the flow velocity well followed the stator vane passage for the entire length of the stator vane.

(a)

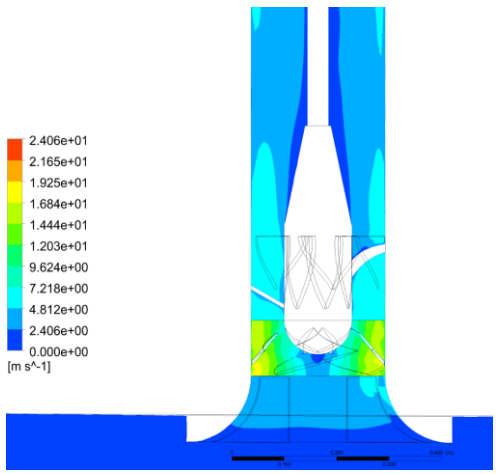

(b)

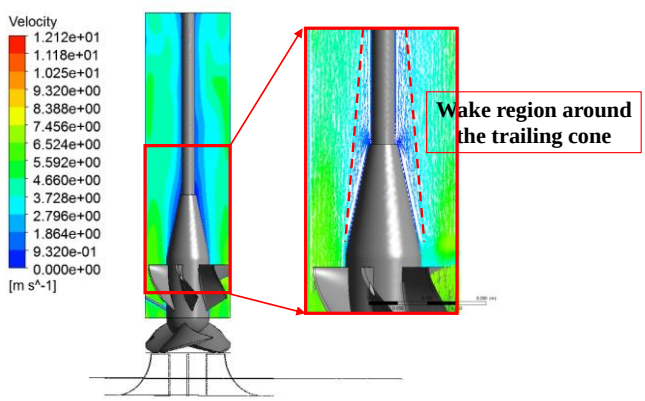

Fig. 8. Flow velocity along the pump system (a) and wake region around the trailing cone (b)

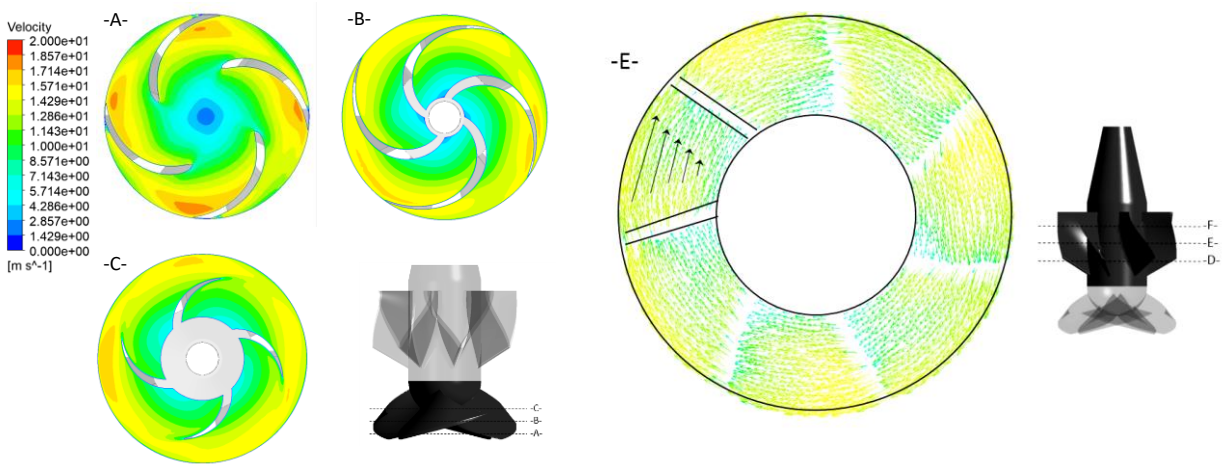

(a) (b)

Fig. 9. Flow field inside the impeller and the stator vane

6. Conclusion

The paper presents the design procedure of an axial flow irrigation pump. It started with the preliminary design which predefined inlet and outlet blade angle of the impeller and the stator vane using a triangular velocity diagram. The efficiency improvement was carried out by repeatedly analyzing the flow structure from CFD and improving the channel profile to reduce the rotational flow structure. The loss of flow energy was found closely related to high velocity gradient in the flow passage. The final version possessed an efficiency at BEP of 75.27% at the delivered head of 5.68 m. with the flow rate of 11,676 L/min. The mild shear layer was observed inside the impeller channel and the trailing cone. Swirling flow kinetic energy downstream from the impeller was well recovered in the stator vane channel.

Nomenclature

C	average flow velocity along annulus flow cross-sectional, m/s
Q	volume flow rate, m^3/s
U	impeller velocity, m/s
ω	angular velocity, rad/s
R	radius, m
η	hydraulic efficiency
ρ	density, kg/m^3
H	height, m
T	torque, N-m
n	shaft speed, rpm
g	gravitational constant, m/s^2
P	power, J/s

Subscripts

a	tip
av	average
i	hub
m	mean
1	rotor leading edge location
2	rotor trailing edge location
X	axial direction

References

[1] Charoensuk J, Asvapoositkul W, Septham K, Wasinarom K, Sanghirun W, Lilavivat V. Development of performance test rig and efficiency improvement of impeller in Thai irrigation pump. Pathumthani: Thailand National Metal and Materials Technology Center; 2019. Report no.:P1851268. (In Thai)

[2] Wasinarom K, Boonchauy D, Noosomton J, Charoensuk J. Improvement of discharge flow structure by bluff-body insert and size reduction of a mixed-flow irrigation pump. J Irrig Drain Eng. 2022;148(3):04021072.

[3] Charoensuk J, Kaewnai S, Jaikuson M, Sanghirun W, Kongtia U, Lilavivat V. Development of a 10-inch irrigation pump for agricultural and drainage purposes. Pathumthani: Thailand National Metal and Materials Technology Center; 2022. Report no.: P2050585. (In Thai)

[4] Ikui T. Flow in axial blade. Bulletin of JSME. 1960;3(9):29-35.

[5] Geerts S. Experimental and numerical study of an axial flow pump [Thesis]. Brussel: Vrije Universiteit Brussel; 2006.

[6] Onisuka K, Ohba H, Munekata M, Yoshikawa H, Terachi H. Studies on the impeller and guide vane of axial-flow pump and shape of suction pipe for pump gate. Proceedings of the 8th International Symposium on Experimental and Computational, Aerothermodynamics of Internal Flows; 2007 July 2-5; Lyon, France.

[7] Singh P, Nestmann F. Axial flow impeller shapes: Part 2. World Pumps. 2011;2011(3):38-41.

[8] Wang WJ, Liang QH, Wang Y, Yang Y, Yin G, Shi XX. Performance analysis of axial flow pump on gap changing between impeller and guide vane. IOP Conf Ser: Mater Sci Eng. 2013;52:032011.

[9] Qian Z, Wang F, Guo Z, Lu J. Performance evaluation of an axial-flow pump with adjustable guide vanes in turbine mode. Renew Energy. 2016;99:1146-1152.

[10] Chen Y, Sun Q, Li Z, Gong Y, Zhai J, Chen H. Numerical study on the energy performance of an axial-flow pump with different wall roughness. Front Energy Res. 2022;10:1-14.

[11] Xu L, Zhang H, Wang C, Ji D, Shi W, Lu W, et al. Hydraulic characteristics of axial flow pump device with different guide vane inlet angles. Front Energy Res. 2022;10:1-13.

[12] Mu T, Zhang R, Xu H, Fei Z, Feng J, Jin Y, et al. Improvement of energy performance of the axial-flow pump by groove flow control technology based on the entropy theory. Energy. 2023;274:12380.